

# Future Changes in Summer Precipitation in Regional Climate Simulations over the Korean Peninsula Forced by Multi-RCP Scenarios of HadGEM2-AO

Dong-Hyun Cha<sup>1</sup>, Dong-Kyou Lee<sup>2</sup>, Chun-Sil Jin<sup>1</sup>, Gayoung Kim<sup>1</sup>, Yonghan Choi<sup>1</sup>, Myoung-Seok Suh<sup>3</sup>, Joong-Bae Ahn<sup>4</sup>, Song-You Hong<sup>5</sup>, Seung-Ki Min<sup>6</sup>, Seong-Chan Park<sup>7</sup>, and Hyun-Suk Kang<sup>8</sup>

<sup>1</sup>School of Urban and Environmental Engineering, Ulsan National Institute of Science and Technology, Ulsan, Korea

<sup>2</sup>School of Earth and Environmental Sciences, Seoul National University, Seoul, Korea

<sup>3</sup>Department of Atmospheric Science, Kongju National University, Kongju, Korea

<sup>4</sup>Department of Atmospheric Sciences, Pusan National University, Busan, Korea

<sup>5</sup>Korea Institute of Atmospheric Prediction Systems, Seoul, Korea

<sup>6</sup>School of Environmental Science and Engineering, Pohang University of Science and Technology, Pohang, Korea

<sup>7</sup>Korea Meteorological Administration, Seoul, Korea

<sup>8</sup>National Institute of Meteorological Science, Jeju, Korea

(Manuscript received 31 October 2015; accepted 1 April 2016)

© The Korean Meteorological Society and Springer 2016

**Abstract:** In this study, the regional climate of the Korean Peninsula (KP) was dynamically downscaled using a high-resolution regional climate model (RCM) forced by multi-representative concentration pathways (RCP) scenarios of HadGEM2-AO, and changes in summer precipitation were investigated. Through the evaluation of the present climate, the RCM reasonably reproduced long-term climatology of summer precipitation over the KP, and captured the sub-seasonal evolution of Changma rain-band. In future projections, all RCP experiments using different RCP radiative forcings (i.e., RCP2.6, RCP4.5, RCP6.0, and RCP8.5 runs) simulated an increased summer precipitation over the KP. However, there were some differences in changing rates of summer precipitation among the RCP experiments. Future increases in summer precipitation were affected by future changes in moisture convergence and surface evaporation. Changing ranges in moisture convergences among RCP experiments were significantly larger than those in surface evaporation. This indicates that the uncertainty of changes in summer precipitation is related to the projection of the monsoon circulation, which determines the moisture convergence field through horizontal advection. Changes in the sub-seasonal evolution of Changma rain-band were inconsistent among RCP experiments. However, all experiments showed that Changma rain-band was enhanced during late June to early July, but it was weakened after mid-July due to the expansion of the western North Pacific subtropical high. These results indicate that precipitation intensity related to Changma rain-band will be increased, but its duration will be reduced in the future.

**Key words:** Climate change, summer precipitation, Korean Peninsula, regional climate model, HadGEM2-AO, multi-RCP scenarios

## 1. Introduction

Recently, high-impact weather and climate events are occurring more frequently with increasing intensities as a result

of climate change (Stocker et al., 2014). In the Korean Peninsula (KP), the frequency and intensity of disastrous weather and climate events such as tropical cyclones, heavy rainfall, drought, and heat wave have changed with global climate change, and their associated damages are gradually increasing. Major natural disasters incurring significant damage in the KP are related to precipitation events such as typhoons, heavy rainfall, and severe snowfall. In order to prepare properly for the future natural disasters in the KP, reliable information on future changes in precipitation is essential.

Most information on future climate change has been based on model scenarios generated by global climate models (GCMs), and dynamical or statistical methods to downscale the GCM's results have been applied to produce detailed estimation of climate change for specific regions of interest. During the summer season in the KP, most precipitation is related to Changma rain-band, one component of East Asian summer monsoon rain-bands (e.g., Maiyu and Baiu bands). In particular, heavy rainfall events associated with meso-scale convective processes frequently occur within East Asian summer monsoon (Lee et al., 2004; Kang et al., 2005; Hong and Lee, 2009; Xu 2013), with occasional torrential rainfall events accompanied by typhoons (Ahn and Lee, 2002; Zhong, 2006; Cha et al., 2011b). Since GCMs cannot resolve such meso-scale meteorological events, statistical downscaling of their results has limitation to reproduce extreme precipitation events. Therefore, a dynamical approach using regional climate models (RCMs), which can resolve small-scale waves embedded within large-scale waves simulated by GCMs, is necessary for the future projection of summer precipitation over the KP (Wang et al., 2004; Hong and Kanamitsu, 2014; Xue et al., 2014).

Recently, Inter-governmental Panels of Climate Change (IPCC) has adopted new scenarios, Representative concentration pathways (RCPs) for its Fifth Assessment Report (AR5). To participate in the Climate Model Inter-comparison

Corresponding Author: Chun-Sil Jin, School of Urban and Environmental Engineering, Ulsan National Institute of Science & Technology, 50 UNIST-gil, Eonyang-eup, Ulju-gun, Ulsan 44919, Korea.  
E-mail: sky80123@gmail.com

Program 5 (CMIP5) with new global climate change scenarios based on RCPs, the National Institute for Meteorological Science/Korea Meteorological Administration (NIMS/KMA) conducted several experiments. As recommended by CMIP5, pre-industrial control run, historical run, and RCP scenarios (2.6, 4.5, 6.0, and 8.5) were performed for long term projection using the coupled global atmosphere-ocean model, Hadley Centre Global Environmental Model version 2-Atmosphere and Ocean (HadGEM2-AO), from the Hadley Centre, the United Kingdom (Baek et al., 2013). The regional climate for the KP has been dynamically downscaled using high-resolution RCMs forced by the RCP scenario of HadGEM2-AO (Lee and Hong, 2014; Hong and Ahn, 2015). Lee and Hong (2014) examined the potential for added value in dynamical downscaling by increasing the spatial resolution of the RCM over the KP. Hong and Ahn (2015) investigated regional summer precipitation changes over the KP for two RCP scenarios (4.5 and 8.5). However, there have been no studies that examine differences in changing rates of summer precipitation in the KP among all available multi-RCP scenarios (2.6, 4.5, 6.0, and 8.5).

To estimate changes in summer precipitation over the KP under four multi-RCP scenarios, we conducted long-term regional climate simulation for the present climate and future climates over the KP and its nearby areas using a high-resolution RCM. The skill of the regional climate simulation was evaluated by comparing the present climate simulation and observation data, and then regional projection (2071-2100) over the KP was estimated. Section 2 explains model configuration and experiments for regional climate simulations. Simulated results were analyzed and described in Section 3. Finally discussions and concluding remarks are given in Section 4.

## 2. Model and experiments

The RCM used in this study is the Seoul National University Regional Climate Model (SNURCM) (Lee et al., 2004), which is based on the National Center for Atmospheric Research Mesoscale Model 5 (NCAR MM5) (Grell et al., 1994). For climate integration, the NCAR Community Land-Surface Model version 3 (CLM3) was coupled to the SNURCM (Bonan et al., 2002) and the spectral nudging technique (von Storch et al., 2000) was employed in the interior domain of the model (Cha and Lee, 2009; Cha et al., 2011a). The physical parameterization schemes used in this study were the Reisner II explicit moisture (Reisner et al., 1998), Kain-Fritsch cumulus convective parameterization (Kain, 2004), YSU planetary boundary layer (Hong et al., 2006), and CCM2 radiation (Briegleb, 1992).

The SNURCM has been applied in a number of studies on the regional climate over East Asia. Lee et al. (2004) reasonably reproduced the record-breaking heavy rainfall over East Asia in the summer of 1998, and Kang et al. (2005) investigated the mechanisms of extreme flood and drought

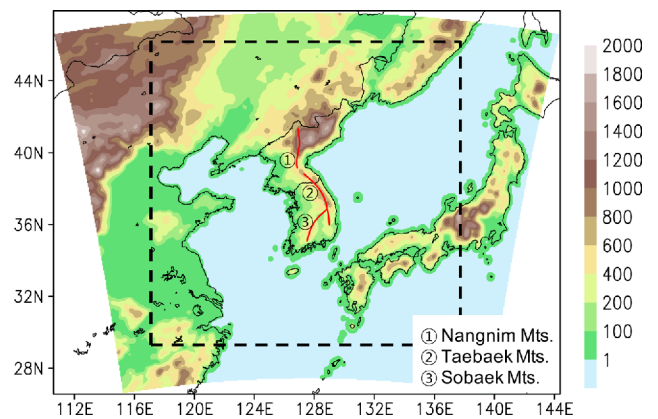


**Fig. 1.** Model domain with topography (m) and mountain ridges (solid lines). Boxed area indicates the analysis zone ( $29^{\circ}$ - $46^{\circ}$ N,  $117^{\circ}$ - $138^{\circ}$ E).

events, and Cha et al. (2011a) examined the impact of local sea surface temperature on East Asian summer monsoon using the SNURCM. In addition, the model was internationally evaluated by participating in the Regional Climate model Inter-comparison Project for Asia (RMIP) (Fu et al., 2005). Recently, Lee et al. (2013) reproduced a high-resolution climate change scenario for East Asia through continuous 70-yr (1980-2049) regional climate simulation with the SNURCM forced by the community climate system model 3 in CMIP3. In addition, the SNURCM has been participated in a project to produce a regional climate change scenario for the East Asian domain of the Coordinated Regional Climate Downscaling Experiment (CORDEX) using multi-models supported by the Korea Meteorological Administration (Suh et al., 2012).

The model domain covers the KP and consists of 200 by 180 grid points along the zonal and meridional directions, respectively, with a horizontal resolution of 12.5 km (Fig. 1). The model uses 24 vertical layers with a top level of 50 hPa. Initial- and boundary-forcing data for driving the regional climate model were obtained from 6-hourly the HadGEM2-AO (Baek et al., 2013) based on historical and four RCP (2.6, 4.5, 6.0, and 8.5) scenarios. The HadGEM2-AO model consists of an atmospheric model with a horizontal resolution of  $1.875^{\circ} \times 1.25^{\circ}$  and 38 vertical levels with an atmospheric top at about 38 km and an ocean model with a 1-degree horizontal resolution and 40 vertical levels. The SNURCM was integrated using the HadGEM2-AO data from January 1979 to December 2010 for present climate, and with four RCP scenarios from January 2019 to December 2100 for future climate. For the period 2006-2010, boundary-forcing data were obtained from RCP8.5 output because the present climate simulation was performed by 2005. Hereafter, the experiment for the present climate is referred to as the Historical run, while the experiments for the future climate using RCP scenarios are referred to as the RCP2.6, RCP4.5, RCP6.0, and RCP8.5 runs according to radiative forcing. A 2-yr spin-up time was applied in both the Historical and RCPs runs. In this

study, simulation results from two time slices representing the present day (1981-2010) and the future (2071-2100) were analyzed.

For the present climate, CO<sub>2</sub> concentrations were derived from a combination of the Law Dome ice core (Etheridge et al., 1998), NOAA global mean data (Conway et al., 1994), and

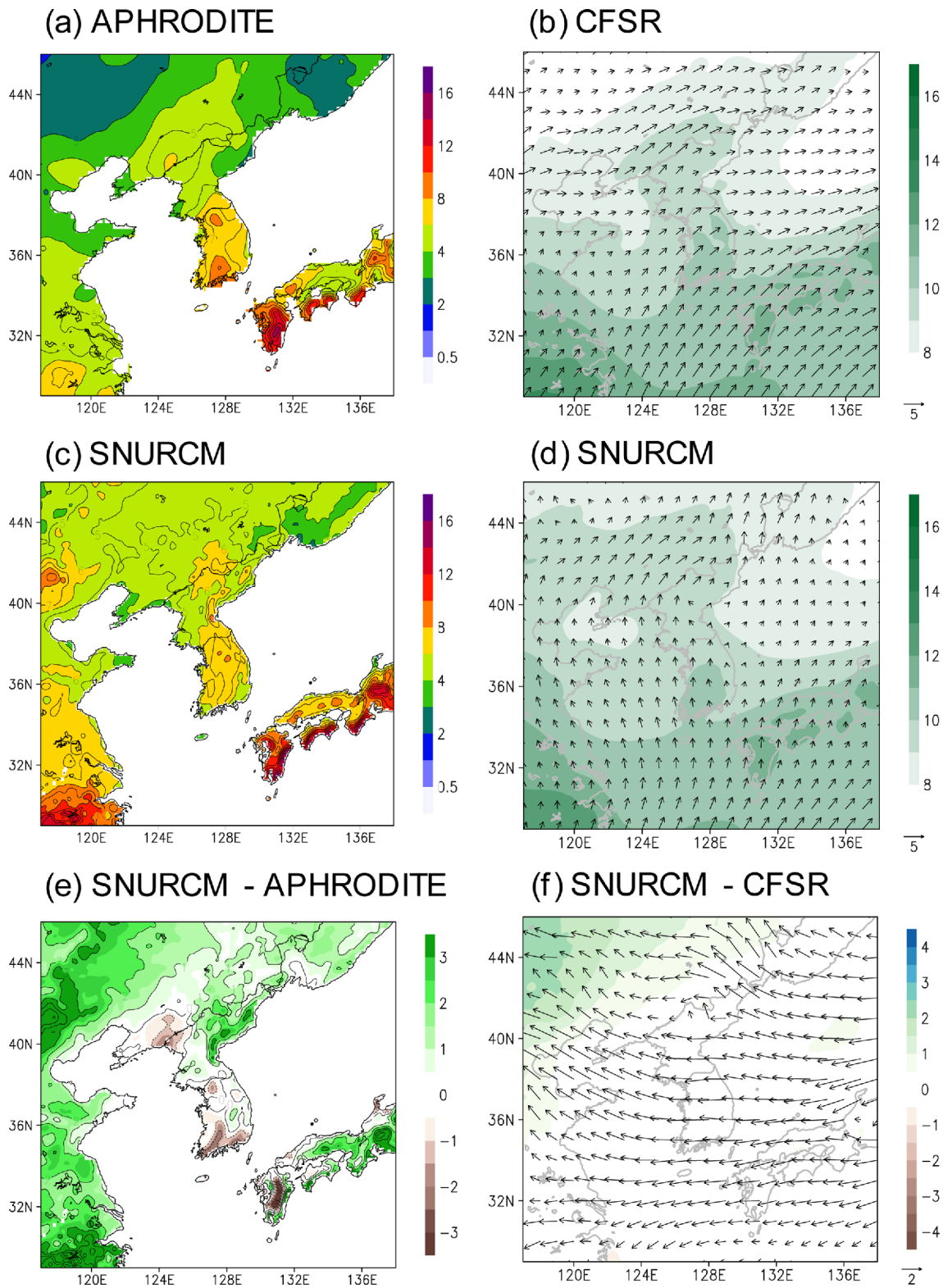


**Fig. 2.** 25-yr (1981-2005) summer mean precipitation (mm d<sup>-1</sup>) (a, c, e) and 850-hPa wind vector (m s<sup>-1</sup>; vector) and 850-hPa specific humidity (g kg<sup>-1</sup>; shading) (b, d, f).

SIO Mauna Kea record (Keeling and Whorf, 2005). For the future climate, CO<sub>2</sub> concentrations were taken from the CMIP5 dataset (Meinshausen et al., 2011). The four RCP scenarios (Moss et al., 2010) are named according to a possible range of global radiative forcing values in 2100 relative to pre-industrial values: peak at  $\sim 3 \text{ W m}^{-2}$  before 2100 followed by decline to  $2.6 \text{ W m}^{-2}$  by 2100 for RCP2.6, stabilizations without overshoot pathways to 6.0 and  $4.5 \text{ W m}^{-2}$  at stabilization after 2100 for RCP6.0 and RCP4.5, respectively, and a rising pathway leading to  $8.5 \text{ W m}^{-2}$  by 2100 for RCP8.5.

In order to evaluate the performance of the model for 1981–2005, the simulated precipitation was compared with the Asian Precipitation-Highly-Resolved Observational Data Integration Towards Evaluation of the Water Resources project (APHRODITE) gridded daily precipitation, which is generated from daily rain gauge data with horizontal resolution of  $0.25^\circ$  (Yatagai et al., 2012). To evaluate simulated synoptic environments including wind and specific humidity, atmospheric variables were obtained from the NCEP climate forecast system reanalysis (CFSR) with a horizontal resolution of  $0.5^\circ$  (Saha et al., 2010). For a convenient comparison, the observations and model results were interpolated to a  $0.1^\circ \times 0.1^\circ$  latitude-longitude grid over the analysis domain (dashed line box in Fig. 1).

### 3. Results

#### a. Evaluation of present model climate in Historical run

In this section, we describe the evaluation of the performance of the SNURCM by comparing the results from Historical run with the observation. Figure 2 shows 25-yr summer mean precipitation and low-level synoptic fields from the observation and Historical run. The spatial pattern of simulated precipitation around the KP is comparable to that of the observation, while precipitation amount over most of the East Asian continent (especially China east coastal region) except for the KP tends to be somewhat overestimated compared to that of the observation. The SNURCM reasonably simulates precipitation amount over central Korea, although it

**Table 1.** Statistics of simulated summer precipitation for the period 1981–2005. Bold values denote significant spatial correlation coefficients at the 99% confidence level based on a Student's *t* test.

Region	Bias	RMSE	Spatial corr.
Korean Peninsula	0.3	1.3	<b>0.56</b>
North Korea	1.0	1.5	<b>0.41</b>
South Korea	−0.5	1.1	<b>0.45</b>

has systematic errors such as overestimation over northeastern Korea (Hamgyong province) and underestimation over south coastal regions (Fig. 2c). The statistics of the 25-yr summer mean precipitation over the KP in Table 1 are also comparable to those from other studies (e.g., Lee et al., 2013; Lee and Hong, 2014; Hong and Ahn, 2015).

Since summer precipitation over East Asia is affected by low-level monsoon circulation and moisture distribution (e.g., Yhang and Hong, 2008; Niu et al., 2015), we compare low-level synoptic fields between the simulation and reanalysis to analyze the cause of the systematic errors of simulated precipitation. In the reanalysis, a warm and wet southwesterly transported from the tropical region to the mid-latitude is dominant over the KP. However, the SNURCM has a systematic error that the dominant low-level wind is southerly rather than southwesterly. This erroneous low-level southerly is associated with that the HadGEM2-AO, large-scale boundary forcing, cannot properly simulate the intraseasonal evolution of the western North Pacific subtropical high (WNPSH), which is considerably related to the East Asian summer monsoon. Same as garbage-in garbage-out as indicated in previous studies (Giorgi and Mearns, 1999; Wang et al., 2004), the systematic error of monsoonal circulation in the large-scale forcing could be inherited by the RCM. In addition, it is possible that the spectral nudging of the wind field applied in this study can augment the propagation of systematic errors from the large-scale forcing. Compared with the reanalysis the SNURCM has easterly bias over most of East Asia as the systematic error of low-level wind (Fig. 2f). This easterly bias leads to dry bias at the low-level and underestimated precipitation over the southern coastal region, namely upstream

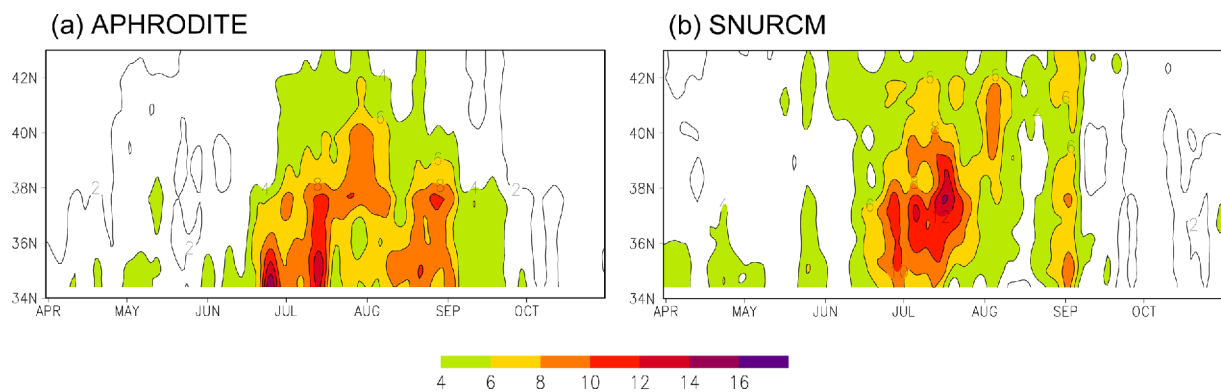


**Fig. 3.** Time-latitude cross-sections of 25-yr (1981–2005) mean daily precipitation ( $\text{mm d}^{-1}$ ), zonal averaged over the Korean Peninsula.

region of the Sobaek Mountains under the observed southwesterly. On the contrary, the circulation bias induces low-level wet bias and overestimated precipitation over northeastern Korea, namely downstream region of the Nangnim Mountains under the observed southwesterly (See Fig. 1 for location). In the same manner, the easterly bias gives rise to low-level wet bias and overestimated precipitation in the China east coastal region.

The SNURCM captures the temporal evolution of Changma rain-band, which significantly contributes to most of the annual precipitation amounts in Korea (Fig. 3). The onset of Changma around late June starting from southern Korea is captured by the SNURCM despite its weak precipitation intensity. This weak intensity is relevant to dry bias over the region caused by an erroneous low-level circulation (i.e., underestimated westerly). It is noted that the model tends to

underestimate precipitation south of 38°N for August compared with the observation. This might be due to the aforementioned systematic error in monsoon circulation as well as weakened activity of tropical cyclones in HadGEM2-AO. As indicated by Ahn and Lee (2002), the regional climate simulation of late summer precipitation over the KP is substantially related to whether tropical cyclones are properly simulated or not. SNURCM forced by HadGEM2-AO tends to underestimate the tropical cyclone activity over the East Asian coastal region because of unfavorable conditions for tropical cyclone activity (e.g., overestimated vertical wind shear) (not shown). In addition, the model domain in this study is too small to completely reproduce the characteristics of tropical cyclones passing through East Asia. Therefore, the simulated tropical cyclones in this study can be generally weaker and less frequent compared with the observation. This unreasonable simulation

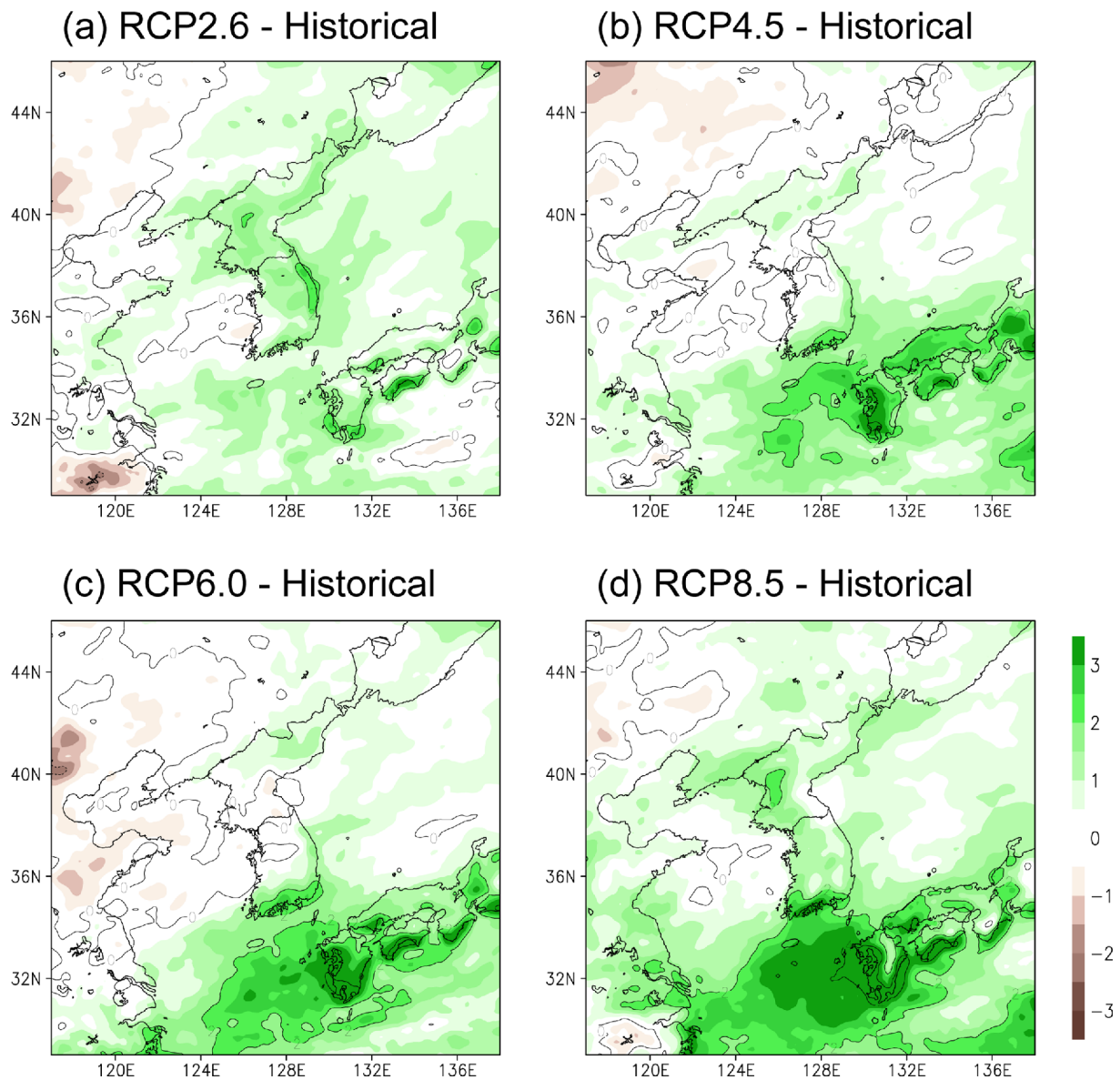


**Fig. 4.** Differences in summer mean precipitation ( $\text{mm d}^{-1}$ ) between future (2071-2100) and present (1981-2010) scenarios.

of tropical cyclone around Korea can result in underestimated precipitation in August. In contrast, precipitation over northern Korea above 38°N tends to be generally overestimated because of the aforementioned wet bias over the downstream region of the Nangnim Mountains.

Despite some systematic errors, the evaluations for the present climate show that the SNURCM has a skill in reproducing regional details embedded in the HadGEM2-AO output for the KP, and therefore, its application in future projections is reasonable.

**b. Future change in summer precipitation**

In this section, we describe an analysis of future change in summer precipitation over the KP by comparing the differences in precipitation and synoptic fields between the four

**Table 2.** Summer precipitation changes averaged over the model domain and KP in future (2071-2100) relative to present (1981-2010) for each RCP run.

	Model domain (Land and Ocean)		Korean Peninsula (Land)	
	Change (mm d <sup>-1</sup> )	Rate of change (%)	Change (mm d <sup>-1</sup> )	Rate of change (%)
RCP2.6	0.58	11.2	1.25	20.5
RCP4.5	0.68	13.1	0.66	10.9
RCP6.0	0.71	13.5	0.61	10.1
RCP8.5	1.19	22.6	1.27	20.9

RCP runs and Historical run. Figure 4 shows differences in summer precipitation between future climatology (2071-2100) and present climatology (1981-2010). Area-averaged precipi-

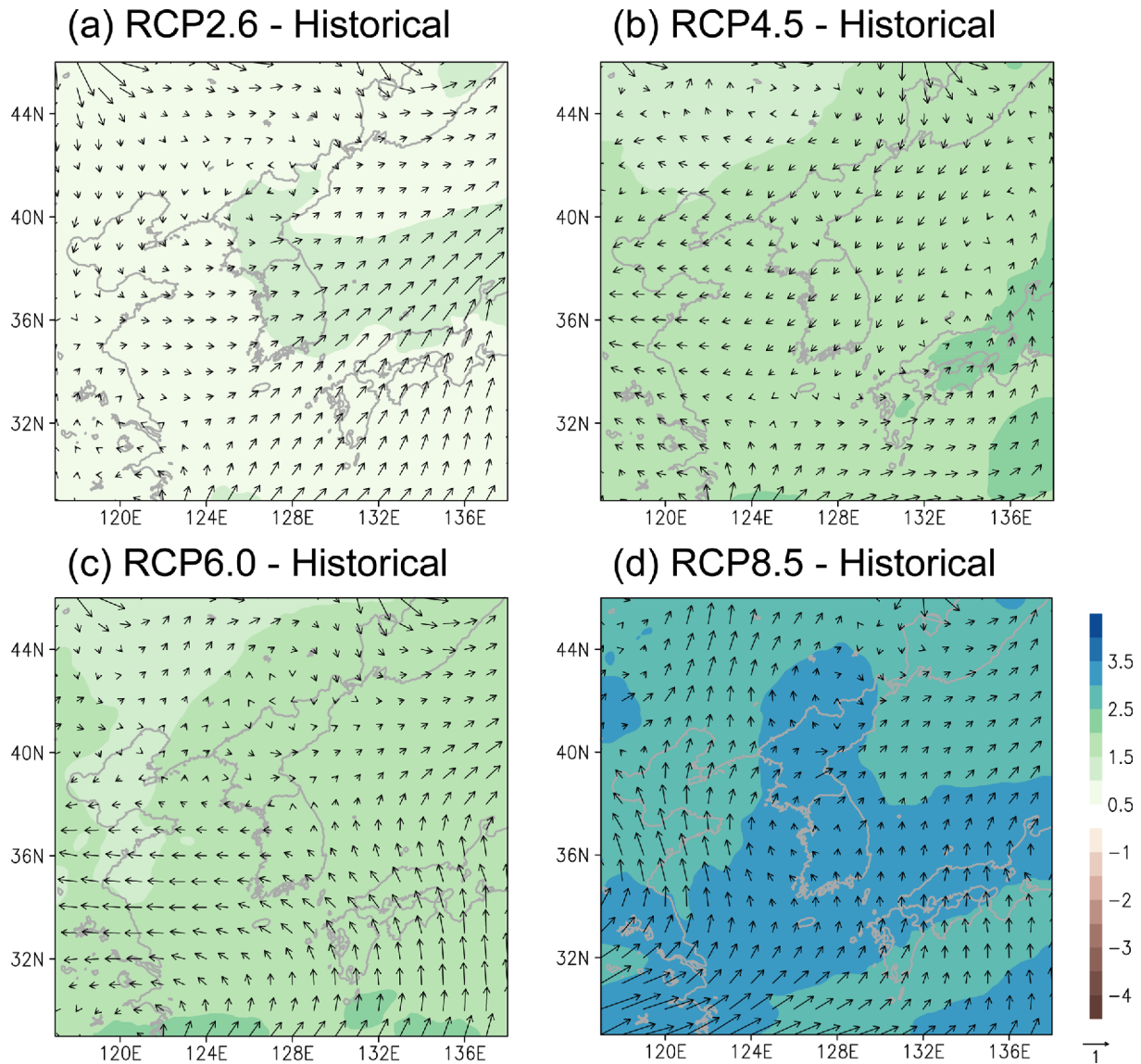


**Fig. 5.** As in Fig. 4, but for 850-hPa wind vector (m s<sup>-1</sup>; vector) and 850-hPa specific humidity (g kg<sup>-1</sup>; shading).

**Table 3.** As in Table 2, but for hydrologic budget averaged over the KP (34–43°N, 124–131°E). C, E, and P indicate moisture convergence, evaporation, and precipitation, respectively. The units are mm d<sup>-1</sup>.

	C	E	P
RCP2.6	0.59	0.30	0.94
RCP4.5	0.15	0.27	0.62
RCP6.0	0.11	0.25	0.57
RCP8.5	0.45	0.32	1.08

tation for the model domain tends to increase in all RCP runs compared with Historical run. The increasing tendency of the amount and changing rate of summer precipitation becomes larger as radiative forcing becomes larger (Table 2). In particular, a linear increasing trend according to RCP radiative forcings is prominent over the ocean. Summer precipitation over the KP also tends to increase in all RCP runs. However, the increasing tendencies are not proportional to RCP radiative forcings. Future summer precipitation over the KP in RCP2.6 and RCP8.5 runs increases by approximately 20%, while that in RCP4.5 and RCP6.0 increases by approximately 10% (Table 2). It is noteworthy that the increasing tendency of summer precipitation over the south coastal region and northern Korea is obvious in all RCP runs, while that over central Korea is uncertain. That is, summer precipitation over central Korea prominently increases in RCP2.6 and RCP8.5, but that in RCP4.5 and RCP6.0 does not change significantly.

To examine the reason for these future changes in summer precipitation over the KP, we analyze changes in low-level synoptic fields (Fig. 5). In all RCP runs, low-level moisture around the KP tends to increase, indicating that the amount of atmospheric water vapor increases with a warming climate due to increased saturation vapor pressure with temperature (Stocker et al., 2014). The increasing tendency of low-level moisture is nearly proportional to RCP radiative forcings. That is, the increase in moisture is the largest (smallest) in RCP8.5 (RCP2.6) run compared to those in other runs. Unlike low-level moisture field, low-level circulation inconsistently changes according to RCP radiative forcings. In RCP2.6 and RCP8.5 runs, the southwesterly or southerly, dominant low-level circulation of the East Asian summer monsoon, is enhanced in the future. On the contrary, differences in the northeasterly and southeasterly are dominant in RCP4.5 and RCP6.0 runs, respectively. This means that different projections of low-level circulation according to dissimilar RCP radiative forcings can lead to differences of moisture advection, which is possibly the major reason for the differences in the projections of future summer precipitation in the RCP runs.

To quantitatively explain the future changes in precipitation over the KP, we analyze the water budget equation (Bosilovich and Sun 1999) around the KP (Table 3).

$$W = C + E - P + R \quad (1)$$

where

$$W = g^{-1} \int_0^1 \frac{\partial p^* q}{\partial t} d\sigma,$$

$$C = -g^{-1} \int_0^1 \nabla \cdot [p^* q V] d\sigma$$

In the water budget equation (1),  $W$ ,  $C$ ,  $E$ ,  $P$ , and  $R$  indicate total change in precipitable water, vertically integrated moisture convergence, evaporation, precipitation, and residual, respectively. Since not only the calculations of  $W$  and  $R$  terms require huge computing resources and data storage but also we focus on the ratios of  $C$  and  $E$  to  $P$ ,  $W$  and  $R$  terms are not considered here. Vertically integrated moisture convergence is derived from 3 hourly instant values of water vapor and wind fields, and is calculated for the region around the KP (34°–43°N, 124°–131°E). The surface evaporation around the KP in the future prominently increases in all RCP runs, and its difference among experiments is not significantly large. However, the change in moisture convergence among RCP runs is notably large. Moisture convergence prominently increases in RCP2.6 and RCP8.5 runs, therefore, the increase in future precipitation in the two runs is more robust compared to those in RCP4.5 and RCP6.0 runs. The increasing moisture convergence in RCP2.6 and RCP8.5 runs is associated with the intensified southwesterly and southerly, respectively, in the future (see Fig. 5). In contrast, the increasing tendencies of moisture convergence in RCP4.5 and RCP6.0 run are relatively small compared with those in others because of the weakened southwesterly. It is noteworthy that the moisture convergences increase in the range of 0.11–0.59 mm d<sup>-1</sup> among the RCP runs, while the surface evaporations increase in the range of 0.25–0.32 mm d<sup>-1</sup>. This indicates that the sensitivity of moisture convergence to RCP radiative forcings is larger than that of surface evaporation and the uncertainty of changes in summer precipitation over the KP is more relevant to the future changes in moisture convergence rather than that of surface evaporation.

In addition, the changes in spatial distribution and temporal variation of Changma rain-band over the KP are inconsistently projected among RCP runs (Fig. 6). The northward shifting of Changma rain-band from the south coastal region to central Korea during late June to mid-July is intensified in all RCP runs. In particular, all runs project more precipitation over the south coastal region around late June and increasing precipitation over the entire KP for August. It should be noted that all runs project the period with decreasing precipitation in July. Consistent with the result of Kusunoki et al. (2006), this can be related to the expanded subtropical high in the future climate resulting in an earlier break of Changma rain with associated downdraft and faster northward marching of the rain-band.

As shown in Fig. 5, the spatial and temporal changes in Changma rain-band could be affected by the temporal evolution of the low-level moisture and circulation change (Fig. 7). All RCP runs simulate an increasing tendency of low-level moisture in the future, which is nearly proportional to RCP radiative forcing. The increasing low-level moisture is signifi-

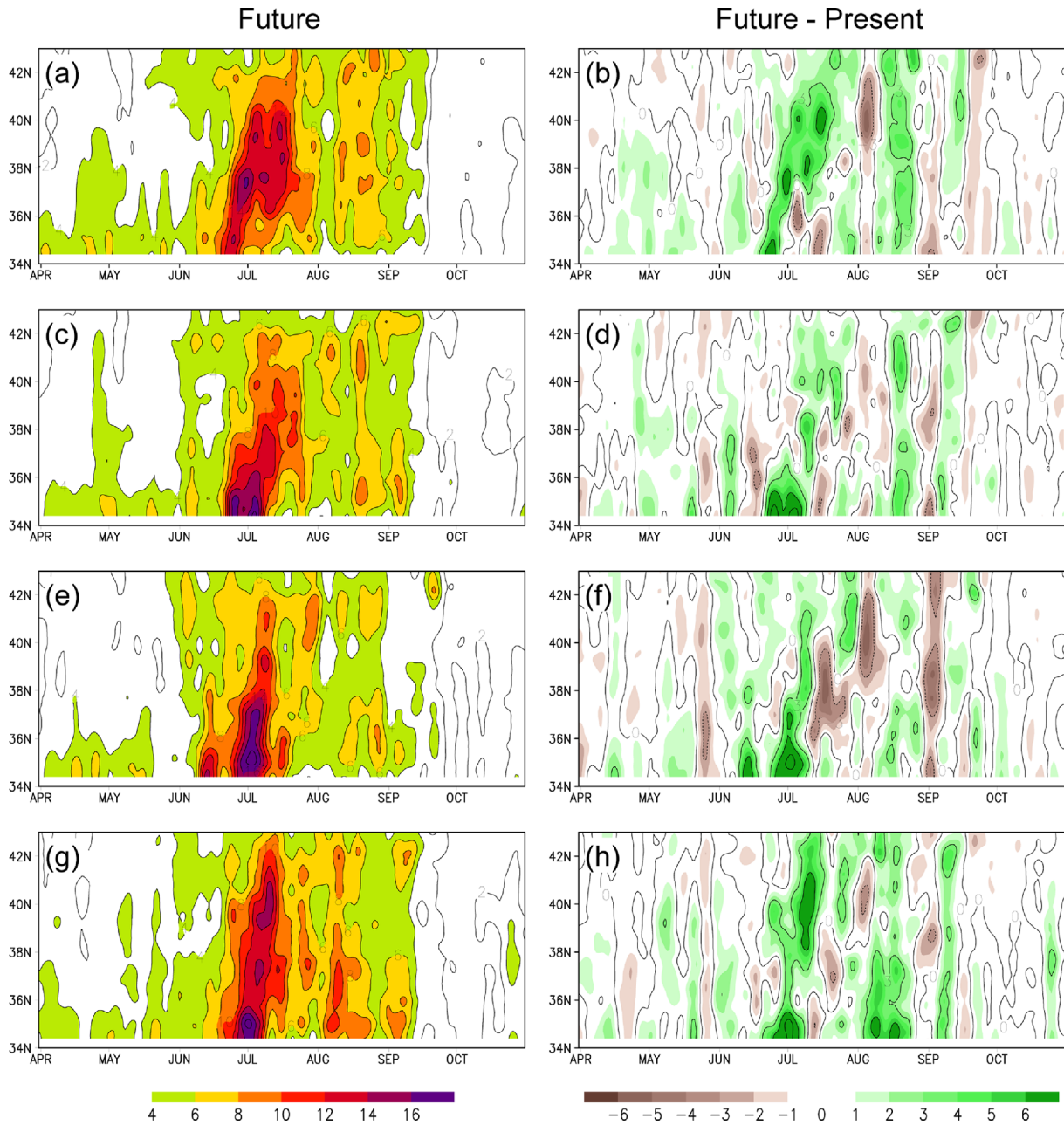


**Fig. 6.** Time-latitude cross-sections of future 30-yr mean daily precipitation (left panels) and its differences (right panels) from present simulation, zonal averaged over the Korean Peninsula.

cantly affected by the changes in surface evaporation and horizontal convergence. Since changes in summer precipitation are more sensitive to horizontal convergence than surface evaporation as shown in Table 3, we further analyze the temporal evolution of changes in low-level circulation. In the RCP2.6, RCP6.0, and RCP8.5 runs, low-level southerly is apparently intensified during most summer season (JJA) except for early June. Even in RCP4.5 run, a southerly is slightly enhanced during the period (late June to mid-July) when Changma rain-band shifts northward. The intensification of the warm and moist southerly from sub-tropical regions leads to

increases in moisture over the KP. From the changes in low-level zonal wind from RCP2.6 and RCP8.5 runs, the enhanced westerly is dominant during late June to early July, and the easterly is noticeably increased after mid-July. A similar change in wind direction is simulated in RCP4.5 and RCP6.0 runs, but it is limited to southern Korea. The change in zonal wind direction can be related to the expansion of the subtropical high in the future. The increasing westerly from late June to early July is because the KP is affected by the southwesterly at the northwestern periphery of enhanced subtropical high. Furthermore, the intensified easterly is associated with the reduced

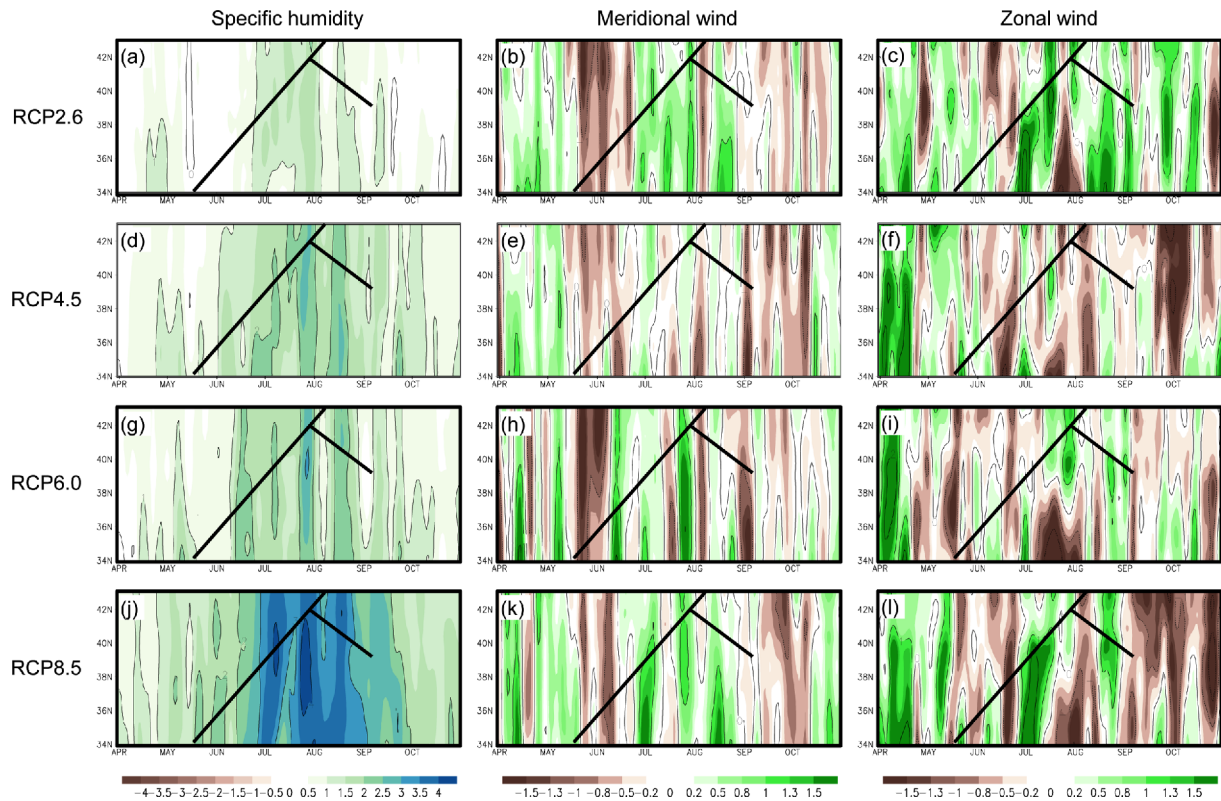


**Fig. 7.** As in Fig. 6, but only for differences in 850-hPa specific humidity (left panels), 850-hPa meridional wind (middle panels), and 850-hPa zonal wind (right panels) between future and present scenarios.

westerly after mid-July when the KP is directly influenced by a huge downdraft inside the subtropical high. Therefore, precipitation relevant to Changma rain-band increases when the westerly is enhanced (i.e., from late June to early July), and then precipitation decreases due to the decreasing westerly under the direct effect of the subtropical high. These results indicate that precipitation intensity related to Changma rain-band will be increased, but its duration will be reduced in the future.

#### 4. Summary and concluding remarks

In this study, regional climate change for the KP was dynamically downscaled using the SNURCM with a 12.5 km horizontal resolution forced by multi RCP scenarios from the HadGEM2-AO, and changes in summer precipitation over the KP for late 21st Century (2071–2100) was investigated. Despite some systematic errors, the SNURCM realistically reproduced present 25-yr mean climatology of summer precipitation over the KP, and reasonably captured the sub-seasonal evolution of Changma rain-band. In the future projection, all RCP runs simulated an increased summer precipitation over the KP. However, there were some differences among the experiments. RCP2.6 and RCP8.5 runs simulated 20% more summer precipitation over the entire KP, while RCP4.5 and RCP6.0 runs simulated 10% increased precipitation particularly over

south coastal region and northern Korea. The increases in summer precipitation over the KP were associated with the increases in surface evaporation and moisture convergence. Surface evaporation tended to similarly increased in all RCP runs, while moisture convergence inconsistently increased with considerable difference among the RCP runs. This indicates that the inconsistent future changes in summer precipitation over the KP among RCP runs were more related to changes in moisture convergence rather than surface evaporation. That is, the uncertainty of changes in summer precipitation can be considerably associated with the projection of the monsoon circulation, which determines the moisture convergence field through horizontal advection. The sub-seasonal evolution of Changma rain-band changed inconsistently among the RCP runs. Nevertheless, all experiments showed that Changma rain-band was enhanced during late June to early July, but it was weakened after mid-July due to the expansion of the subtropical high.

This study showed that future changes in summer precipitation over the KP could be different among experiments with dissimilar RCP scenarios, and such differences were affected by the monsoon circulation. These results indicate that RCM should realistically simulate the spatial distribution and temporal variation of the monsoon circulation and subtropical high before it is applied to future regional climate projections for the KP. One limitation of this study is that global climate

change scenarios generated by single GCM (i.g., HadGEM2-AO) were deterministically downscaled using single RCM (i.e., SNURCM), which possibly results in large uncertainties. To overcome the limitation, the uncertainties of future regional climate projections should be reduced through multi-models ensemble approach in which global scenarios from multi-GCMs are dynamically downscaled with multi-RCMs.

**Acknowledgements.** This work was funded by the Korea Meteorological Administration Research and Development Program under Grant KMIPA 2015-2083.

**Edited by:** Jimy Dudhia

### References

- Ahn, Y. I., and D. K. Lee, 2002: Impact of bogus tropical cyclones on summertime circulation in regional climate simulation. *J. Geophys. Res.-Atmos.*, **107**, ACL 8-1-ACL 8-16.
- Baek, H. J., and Coauthors, 2013: Climate change in the 21st century simulated by HadGEM2-AO under representative concentration pathways. *Asia-Pac. J. Atmos. Sci.*, **49**, 603-618.
- Bonan, G. B., K. W. Oleson, M. Vertenstein, S. Levis, X. B. Zeng, Y. J. Dai, R. E. Dickinson, and Z. L. Yang, 2002: The land surface climatology of the community land model coupled to the NCAR community climate model. *J. Climate*, **15**, 3123-3149.
- Bosilovich, M. G., and W. Y. Sun, 1999: Numerical simulation of the 1993 midwestern flood: Land-atmosphere interactions. *J. Climate*, **12**, 1490-1505.
- Briegleb, B. P., 1992: Delta-eddington approximation for solar-radiation in the NCAR community climate model. *J. Geophys. Res.*, **97**, 7603-7612.
- Cha, D. H., and D. K. Lee, 2009: Reduction of systematic errors in regional climate simulations of the summer monsoon over East Asia and the western North Pacific by applying the spectral nudging technique. *J. Geophys. Res.-Atmos.*, **114**, D14108, doi:10.1029/2008jd011176.
- \_\_\_\_\_, C. S. Jin, and D. K. Lee, 2011a: Impact of local sea surface temperature anomaly over the western North Pacific on extreme East Asian summer monsoon. *Clim. Dynam.*, **37**, 1691-1705.
- \_\_\_\_\_, \_\_\_\_\_, \_\_\_\_\_, and Y. H. Kuo, 2011b: Impact of intermittent spectral nudging on regional climate simulation using Weather Research and Forecasting model. *J. Geophys. Res.-Atmos.*, **116**, D10103, doi:10.1029/2010jd015069.
- Conway, T. J., P. P. Tans, L. S. Waterman, and K. W. Thoning, 1994: Evidence for Interannual Variability of the Carbon-Cycle from the National-Oceanic-and-Atmospheric-Administration Climate-Monitoring-and-Diagnostics-Laboratory Global-Air-Sampling-Network. *J. Geophys. Res.-Atmos.*, **99**, 22831-22855.
- Etheridge, D. M., L. P. Steele, R. L. Langenfelds, R. J. Francey, J. M. Barnola, and V. I. Morgan, 1998: Historical CO<sub>2</sub> records from the Law Dome DE08, DE08-2, and DSS ice cores. *Trends: a compendium of data on global change*, 351-364.
- Fu, C. B., S. Y. Wang, Z. Xiong, W. J. Gutowski, D. K. Lee, J. L. McGregor, Y. Sato, H. Kato, J. W. Kim, and M. S. Suh, 2005: Regional climate model intercomparison project for Asia. *Bull. American Meteorol. Soc.*, **86**, 257-266.
- Giorgi, F., and L. O. Mearns, 1999: Introduction to special section: Regional climate modeling revisited. *J. Geophys. Res.-Atmos.*, **104**, 6335-6352.
- Grell, G. A., J. Dudhia, and D. R. Stauffer, 1994: A description of the fifth-generation Penn State/NCAR mesoscale model (MM5). NCAR/TN-398+STR, NCAR Technical Note, 122 pp.
- Hong, J. Y., and J. B. Ahn, 2015: Changes of Early Summer Precipitation in the Korean Peninsula and Nearby Regions Based on RCP Simulations. *J. Climate*, **28**, 3557-3578.
- Hong, S. Y., Y. Noh, and J. Dudhia, 2006: A new vertical diffusion package with an explicit treatment of entrainment processes. *Mon. Wea. Rev.*, **134**, 2318-2341.
- \_\_\_\_\_, and J. W. Lee, 2009: Assessment of the WRF model in reproducing a flash-flood heavy rainfall event over Korea. *Atmos. Res.*, **93**, 818-831.
- \_\_\_\_\_, and M. Kanamitsu, 2014: Dynamical downscaling: Fundamental issues from an NWP point of view and recommendations. *Asia-Pac. J. Atmos. Sci.*, **50**, 83-104.
- Kain, J. S., 2004: The Kain-Fritsch convective parameterization: An update. *J. Applied Meteorology*, **43**, 170-181.
- Kang, H. S., D. H. Cha, and D. K. Lee, 2005: Evaluation of the mesoscale model/land surface model (MM5/LSM) coupled model for East Asian summer monsoon simulations. *J. Geophys. Res.-Atmos.*, **110**, D10105, doi:10.1029/2004jd005266.
- Keeling, C. D., and T. P. Whorf, 2005: Atmospheric CO<sub>2</sub> records from sites in the SIO air sampling network. *Trends: a compendium of data on global change*, 16-26.
- Kusunoki, S., J. Yoshimura, H. Yoshimura, A. Noda, K. Oouchi, and R. Mizuta, 2006: Change of Baiu rain band in global warming projection by an atmospheric general circulation model with a 20-km grid size. *J. Meteor. Soc. Japan*, **84**, 581-611.
- Lee, D. K., D. H. Cha, and H. S. Kang, 2004: Regional climate simulation of the 1998 summer flood over East Asia. *J. Meteor. Soc. Japan*, **82**, 1735-1753.
- \_\_\_\_\_, \_\_\_\_\_, C. S. Jin, and S. J. Choi, 2013: A regional climate change simulation over East Asia. *Asia-Pac. J. Atmos. Sci.*, **49**, 655-664.
- Lee, J. W., and S. Y. Hong, 2014: Potential for added value to downscaled climate extremes over Korea by increased resolution of a regional climate model. *Theor. Appl. Climatol.*, **117**, 667-677.
- Meinshausen, M., S. J. Smith, K. Calvin, J. S. Daniel, M. Kainuma, J. Lamarque, K. Matsumoto, S. Montzka, S. Raper, and K. Riahi, 2011: The RCP greenhouse gas concentrations and their extensions from 1765 to 2300. *Climatic Change*, **109**, 213-241.
- Moss, R. H., J. A. Edmonds, K. A. Hibbard, M. R. Manning, S. K. Rose, D. P. Van Vuuren, T. R. Carter, S. Emori, M. Kainuma, and T. Kram, 2010: The next generation of scenarios for climate change research and assessment. *Nature*, **463**, 747-756.
- Niu, X., S. Wang, J. Tang, D. K. Lee, X. Gao, J. Wu, S. Hong, W. J. Gutowski, and J. McGregor, 2015: Multimodel ensemble projection of precipitation in eastern China under A1B emission scenario. *J. Geophys. Res.-Atmos.*, **120**, 9965-9980.
- Reisner, J., R. Rasmussen, and R. Bruintjes, 1998: Explicit forecasting of supercooled liquid water in winter storms using the MM5 mesoscale model. *Q. J. Roy. Meteor. Soc.*, **124**, 1071-1108.
- Saha, S., S. Moorthi, H.-L. Pan, X. Wu, J. Wang, S. Nadiga, P. Tripp, R. Kistler, J. Woollen, and D. Behringer, 2010: The NCEP climate forecast system reanalysis. *Bull. American Meteorol. Soc.*, **91**, 1015-1057.
- Stocker, T. F., and Coauthors, Eds., 2014: *Climate change 2013: The physical science basis*. Cambridge University Press, 1535 pp.
- Suh, M. S., S. G. Oh, D. K. Lee, D. H. Cha, S. J. Choi, C. S. Jin, and S. Y. Hong, 2012: Development of New Ensemble Methods Based on the Performance Skills of Regional Climate Models over South Korea. *J. Climate*, **25**, 7067-7082.
- von Storch, H., H. Langenberg, and F. Feser, 2000: A spectral nudging technique for dynamical downscaling purposes. *Mon. Wea. Rev.*, **128**, 3664-3673.
- Wang, Y. Q., L. R. Leung, J. L. McGregor, D. K. Lee, W. C. Wang, Y. H. Ding, and F. Kimura, 2004: Regional climate modeling: Progress,

- challenges, and prospects. *J. Meteor. Soc. Japan*, **82**, 1599-1628.
- Xu, W. X., 2013: Precipitation and Convective Characteristics of Summer Deep Convection over East Asia Observed by TRMM. *Mon. Wea. Rev.*, **141**, 1577-1592.
- Xue, Y. K., Z. Janjic, J. Dudhia, R. Vasic, and F. De Sales, 2014: A review on regional dynamical downscaling in intraseasonal to seasonal simulation/prediction and major factors that affect downscaling ability. *Atmos. Res.*, **147**, 68-85.
- Yatagai, A., K. Kamiguchi, O. Arakawa, A. Hamada, N. Yasutomi, and A. Kitoh, 2012: APHRODITE Constructing a Long-Term Daily Gridded Precipitation Dataset for Asia Based on a Dense Network of Rain Gauges. *Bull. American Meteorol. Soc.*, **93**, 1401-1415.
- Yhang, Y. B., and S. Y. Hong, 2008: Improved physical processes in a regional climate model and their impact on the simulated summer monsoon circulations over East Asia. *J. Climate*, **21**, 963-979.
- Zhong, Z., 2006: A possible cause of a regional climate model's failure in simulating the east Asian summer monsoon. *Geophys. Res. Lett.*, **33**, L24707, doi:10.1029/2006GL027654.